

Removal of bovine serum albumin using solid-phase extraction with *in-situ* polymerized stationary phase in a microfluidic device

Eun Zoo Lee^a, Yun Suk Huh^a, Young-Si Jun^a, Hyo Jin Won^a, Yeon Ki Hong^b,
Tae Jung Park^{a,c}, Sang Yup Lee^{a,c,d}, Won Hi Hong^{a,*}

^a Department of Chemical and Biomolecular Engineering (BK21 program), KAIST, 335 Gwahangno, Yuseong-gu, Daejeon 305-701, South Korea

^b Department of Chemical and Biological Engineering, Chungju National University, 72 Daehak-ro, Chungju, Chungbuk 380-702, South Korea

^c BioProcess Engineering Research Center, Center for Systems and Synthetic Biotechnology, Institute for the BioCentury, Center for Ultramicrochemical Process Systems, KAIST, 335 Gwahangno, Yuseong-gu, Daejeon 305-701, South Korea

^d Department of Bio and Brain Engineering, and Bioinformatics Research Center, KAIST, 335 Gwahangno, Yuseong-gu, Daejeon 305-701, South Korea

Received 29 November 2007; received in revised form 17 January 2008; accepted 28 January 2008

Available online 13 February 2008

Abstract

Serum albumin, one of the most abundant serum proteins, blocks the expression of other important biomarkers. The objective of this study is to remove serum albumin effectively by using solid-phase extraction (SPE) in microfluidic devices. Photo-polymerized adsorbent as a stationary phase of SPE was used to remove bovine serum albumin (BSA). The adsorption capacity was examined with the effect of pH and concentration in BSA solution, and adjustment of monomer concentration such as hydrophilic 2-acrylamido-2-methyl-1-propanesulfonic acid and acrylamide in the adsorbent. The effect of hydrophobic butyl methacrylate on BSA adsorption was also studied. Selective removal in a bicomponent with BSA and bovine γ -globulin was performed by adjusting the pH as required.

© 2008 Elsevier B.V. All rights reserved.

Keywords: Bovine serum albumin; *In-situ* photo-polymerization; Solid-phase extraction; Microfluidic device; Sample preparation

1. Introduction

In the last several years, there has been heightened interest in the proteome of both serum and plasma. The composition of the serum protein can reflect the physiological and pathophysiological state of the status of the human body and is influenced by the status of many different organ systems. Serum proteins may also undergo disease-induced changes [1]. Therefore, these proteins have potential to act as biomarkers to detect disease, monitor disease progression, and assess the clinical status of patients. However, albumin and immunoglobulin which constitute about 60–97% of the total serum protein usually hinder the detection of other proteins that are diagnostically significant and present at far lower concentrations. Removal of abundant serum protein would increase the intensity informative disease markers

that exist in low concentrations. Numerous attempts have been made to separate serum albumin from human plasma for more accurate analysis by biomarkers; techniques used to this purpose include affinity chromatography, isoelectric trapping and ultrafiltration. In the present study, solid-phase extraction (SPE) was selected to separate serum albumin.

SPE is widely used for the isolation and concentration of target analytes as well as the clean-up of samples in pharmaceutical, clinical and environmental application and in food chemistry [2,3]. SPE was initially developed to replace the liquid–liquid extraction (LLE). The LLE system consumes relatively large amount of high-purity solvents with expensive disposal requirements. In addition, it is difficult to automate and labor intensive. In contrast, SPE benefits from low intrinsic costs, shorter processing times, low solvent consumption and simpler processing procedures [4]. There are two types of SPE. The first type involves fiber coating with modification which has various affinities. These fibers are dipped into the solutions and the target materials are extracted. This technique is typically used in the

* Corresponding author. Tel.: +82 42 869 3919; fax: +82 42 869 3910.
E-mail address: whhong@kaist.ac.kr (W.H. Hong).

determination of pesticide residues in food and detection of contaminants in water [5,6]. The other type of SPE involves stationary phase packing. This approach can be divided into two types on the basis of whether a frit is used to support the packing materials. The frit-structured method generally uses glass fiber to support packing materials or a weir is fabricated in the device [7]. The fabrication of frit in the microchannel is complicated. Therefore, a fritless method was used in this study. Among the fritless methods, a simply modified channel can be used. Moreover, an *in-situ* photo-polymerized stationary phase can be used to increase the contact area between the adsorbate and the adsorbent. In the early 1990s, Fréchet et al. introduced macroscopic rigid porous monoliths prepared *in-situ* by a thermally initiated polymerization process [8–11]. However, the free-radical polymerization initiated by heat used originally is not proper for the preparation of monolithic structures within a microchip. Thus, a UV-initiated polymerization process was used similar to the standard photolithography used for patterning in microelectronics. This enables the formation of stationary phase only within a specified region of the microfluidic device [12]. Using a mask, the polymerization may be strictly confined within areas exposed to radiation while no polymerization is observed in dark areas.

In this study, BSA was removed using SPE that has an *in-situ* photo-polymerized stationary phase, as a fritless method in microchannel, to perform a sample preparation on a chip level. The polymerized adsorbent was characterized with BET/porosimetry, IR, scanning electron microscopy (SEM), and elemental analysis. Adsorption isotherms of polymerized adsorbents were obtained to investigate an adsorption capacity. Effect of pH on BSA adsorption onto polymerized adsorbent was also observed. Kim et al. investigate a batch separation that BSA was adsorbed on microspheres that polymerized using soap-free emulsion method while an adsorption of bovine hemoglobin was minimized at adjusted pH [13]. In this paper, BSA was selectively adsorbed on *in-situ* photo-polymerized stationary phase with adjustment of pH from binary protein solution of BSA and bovine γ -globulin (BGG) in microfluidic device.

2. Experimental

2.1. Materials

2.1.1. Stationary phase in SPE system

Ethylene glycol dimethacrylate (EGDMA) and butyl methacrylate (BMA) were purchased from Sigma–Aldrich (St. Louis, MO, USA). 2-Acrylamido-2-methyl-1-propanesulfonic acid (AMPS) and acrylamide (AAM) were obtained from Aldrich. EGDMA and BMA were purified with alumina powder [14]. 2,2-Dimethoxy-2-phenyl-acetophenone (DPA, Aldrich) was used as an initiator for the photo-polymerization of the stationary phase. Ethanol and methanol (Merck) were used as porogenic solvents.

2.1.2. Model proteins

BSA (Sigma) was used as a model protein. γ -Globulin from bovine was purchased from Sigma. A 0.1 M acetic buffer, a mixture of sodium acetate (Sigma–Aldrich) and acetic acid (Junsei), was used.

Table 1

Composition of the monomer solutions (porogenic solvents: methanol 35.72 μ l, ethanol 17.86 μ l, initiator: DPA 0.5 mg)

Polymer	EGDMA (μ l)	BMA (μ l)	AMPS (mg)	AAM (mg)
S1	9.92		0.518	
S2	9.92		1.036	
S3	9.92		2.072	
S4	9.92		4.145	
BS1	9.92	7.94	0.518	
BS3	9.92	7.94	2.072	
M1	9.92			
M2	9.92			
M3	9.92			
M4	9.92			3.554
BM3	9.92	7.94		1.777

2.1.3. Microfluidic device

SU-8 100 photoresist and developer were purchased from Microchem (Newton, MA, USA), and 4 in. silicon wafers were obtained from LG Siltron Inc. (Incheon, South Korea) The wafers were used in the softlithography process as a fabrication master of the microfluidic devices. Polydimethylsiloxane was purchased from Dow Corning (Midland, MI, USA) and slide glass from Knittle Glaser (Braunschweig, Germany). The microfluidic device was fabricated by soft-lithography and a replica molding method. The dimension of stationary phase part is 1.0 cm (length) \times 0.5 cm (width) \times 50 μ m (depth). The channel size linking an inlet or outlet to stationary phase is 1 cm (length) \times 500 μ m (width) \times 50 μ m (depth).

2.2. Methods

For preparation of *in-situ* photo-polymerized adsorbent in microchannel, the monomer solutions were mixed with the composition as shown in Table 1. The monomer solution was pumped into the channel and exposed a UV light source of 365 nm to a back-side of microchannel for 15 min. UV exposure intensity could be uniformed with exposure to back-side of microchannel which is a glass. After the polymerization reaction, the channel was washed with methanol to remove the unreacted monomers and porogenic solvent [15].

Equilibrium study was conducted off-chip to investigate the capacity of photo-polymerized adsorbent. One gram of adsorbent and 20 mL of BSA solution were mixed and stirred at 25 $^{\circ}$ C for 12 h. After equilibrium, a 1 mL sample was withdrawn from the aqueous phase, centrifuged at 5000 rpm for 10 min. SPE in microfluidic device was carried out with same ratio of amount of *in-situ* photo-polymerized adsorbent to BSA solution.

The protein concentrations of the samples were determined by the Bradford method. The absolute value of absorbance was obtained by using a UV/visible spectrophotometer. When using the Bradford method, calibration is necessary for each experimental condition. BSA calibration was performed in sodium acetate buffer, changing the concentration of BSA from 0 to 2 mg/mL. BSA concentration was determined on the basis of this calibration. In this experiment, Pro-measure solution from Intron Biotechnology (Seongnam, South Korea), a commercial kit for the Bradford method, was used.

2.3. Characterization of photo-polymerized adsorbent

The characterization of photo-polymerized adsorbents was performed after taking off from the microchannel. The pore size distribution was determined using an Autopore IV 9500 mercury intrusion porosimeter. The specific surface area was calculated from the BET isotherms of nitrogen adsorption and desorption using a Tristar 3000. SEM images were obtained by a field emission SEM system (Philips SEM 535M) equipped with a Schottky based field emission gun. The functional group of the polymerized stationary phase was confirmed using a Jasco (Tokyo, Japan) FT-IR instrument Model 4100 in the attenuated total reflection (ATR) mode. Elemental analysis of polymerized adsorbent was performed using a Vario EL 3 elemental analyzer manufactured by Elementar (Hanau, Germany). The purified proteins were analyzed by sodium dodecyl sulfate-polyacrylamide gel electrophoresis (SDS-PAGE). Proteins were separated in 10% acrylamide gel and visualized by Coomassie brilliant blue staining. Molecular sizes of the model proteins were analyzed by comparison with an SDS-PAGE standard marker.

3. Results and discussion

3.1. Characterization of photo-polymerized stationary phase

EGDMA, BMA, AMPS, and AAm were polymerized in various ratios with a constant amount of porogenic solvents, which are responsible for the pore formation. In spite of the composition change in the monomer solution, the pore size was in a range of 90–100 nm. Specific surface area was in a range of 3–4 m²/g. SEM images of the polymerized adsorbent are shown in Fig. 1. As shown in Fig. 1, the stationary phase was polymerized as spherical shape. It was confirmed that the particle size was about 2 μm. In the case of polymerized adsorbent with AMPS and AAm, each polymer has functional group of SO₂ or NH₂. As shown in Fig. 2, S=O was confirmed at 1000 cm⁻¹ and NH₂ was confirmed at 3650 cm⁻¹ [16].

3.2. Effect of pH on BSA adsorption

The effect of pH on BSA adsorption is shown in Fig. 3. The isoelectric point of BSA is about 4.9. Upon deviation from the isoelectric point, the adsorbed amount of the protein was decreased drastically. This observation accords with the results of some other researchers, where the maximum adsorption from aqueous protein solutions was usually observed at the isoelectric point [17]. The maximum adsorption was shifted to the acidic or basic region from the isoelectric point of BSA by addition of a ternary monomer such as AMPS and AAm. As shown in Fig. 3, in the case of a sulfonated adsorbent, the maximum adsorbed amount was observed at a slightly acidic condition due to the electrostatic interaction between negatively charged adsorbent and positively charged BSA molecules. In the case of aminated adsorbent, the maximum adsorbed amount was observed at a little higher pH value than isoelectric point because of the

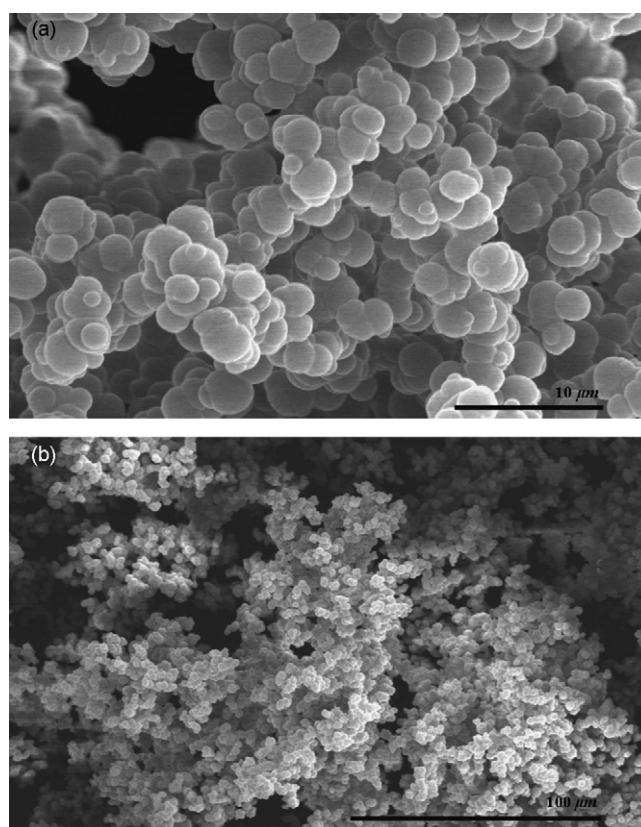


Fig. 1. Scanning electron microscope images of photo-polymerized adsorbent.

electrostatic interaction between positively charged adsorbent and negatively charged BSA molecules. The schematic diagram of the interaction between protein molecules and polymerized adsorbent, and microfluidic device were shown in Fig. 4. The decrease of adsorbed amount may be caused by the lateral electrostatic repulsions between adjacent adsorbed BSA molecules when deviating from isoelectric point. For the same polymerized adsorbent at different pH, there are some contradictory factors in the adsorption process: the charged BSA molecule is favorable because of the oppositely charged polymerized adsorbent. How-

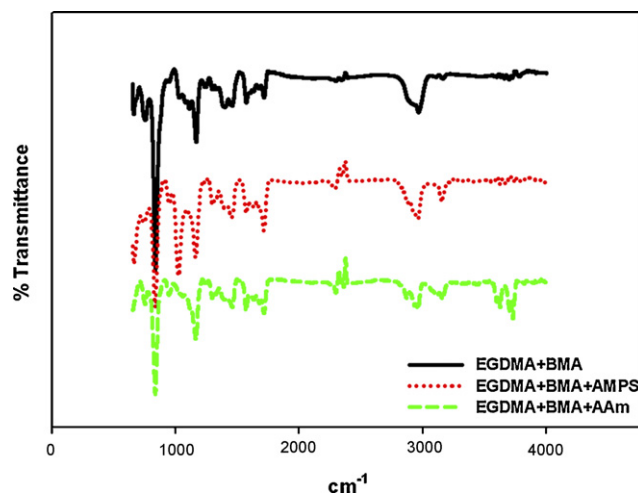


Fig. 2. IR spectra of polymerized stationary phase.

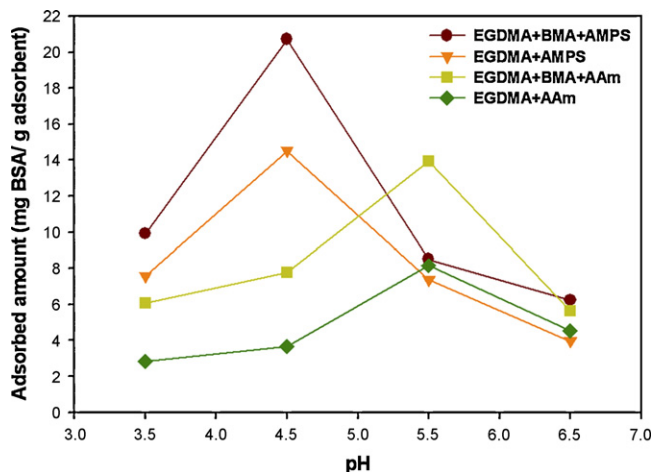


Fig. 3. BSA adsorption onto the polymerized adsorbents with the effect of pH at room temperature (concentration of BSA solution: 1 mg/mL).

ever, the net charge of the BSA molecule adsorbed on the surface of polymerized adsorbent would hinder the further adsorption. The electrostatic and steric impulsion resulting from net charge of BSA would counteract the attractive interaction between the adsorbent surface and the BSA molecules.

The pH that was determined by these experiments will be used in the experiments for the adsorption isotherms. Further experiments were performed at pH 4.5 and pH 5.5 with copolymerized adsorbents AMPS and AAm, respectively.

3.3. Effect of hydrophilic interaction on BSA adsorption

Fig. 5 shows the adsorption isotherms, which were fitted to the Freundlich, Langmuir, and Langmuir–Freundlich (Sips) model using the nonlinear regression method. The equations of the

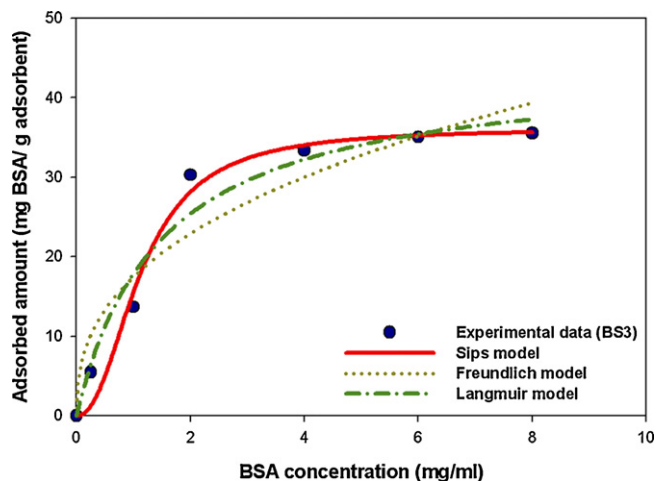


Fig. 5. Adsorption isotherms fitted to Freundlich, Langmuir and Sips models.

adsorption models are as follows:

$$\text{Freundlich: } q_s = KC_b^{1/n} \quad (1)$$

$$\text{Langmuir: } q_s = q_m \frac{KC_b}{1 + KC_b} \quad (2)$$

$$\text{Langmuir–Freundlich (Sips): } q_s = q_m \frac{KC_b^{1/n}}{1 + KC_b^{1/n}} \quad (3)$$

where C_b is the bulk concentration, and q_m and q_s denote the maximum adsorbed amount and the amount of adsorption at a certain BSA concentration. K is the adsorption constant and n is the exponential factor. In the Langmuir–Freundlich model, the values of n were relatively constant between 0.4 and 0.5, and hence n could be fixed to its average value of 0.45 [18]. This is similar to hydrocarbon adsorption on activated carbon [19],

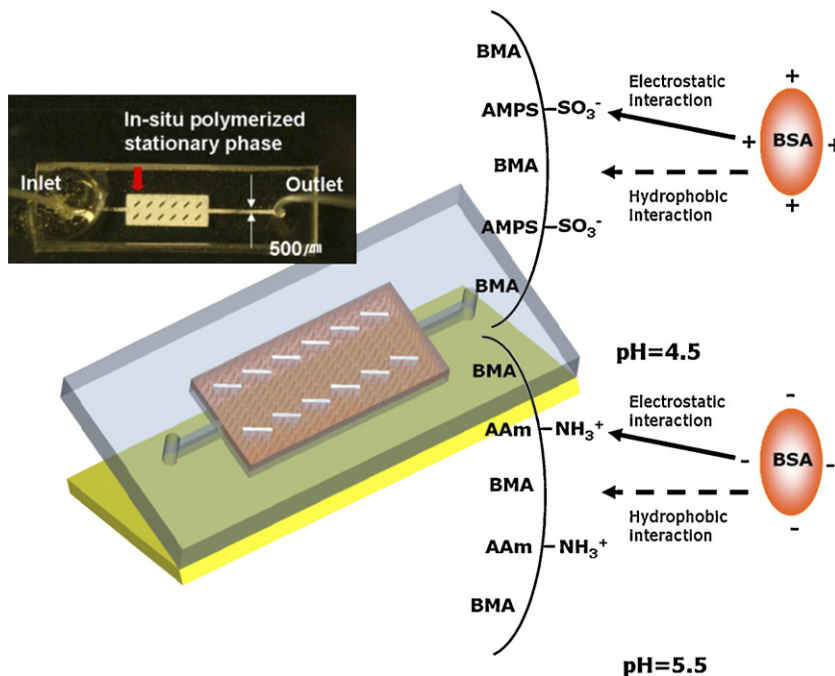


Fig. 4. Schematic diagram of the microfluidic device and the interaction between protein molecules and polymerized adsorbent.

Table 2
 n , q_m , K and R^2 values for BSA adsorption on polymerized adsorbents

Polymer	Adsorption model								
	Freundlich			Langmuir			Langmuir–Freundlich (Sips)		
	n	K	R^2	q_m	K	R^2	q_m	K	R^2
S1	4.54	10.97	0.857	17.64	1.96	0.943	15.81	4.61	0.978
S2	3.95	12.52	0.879	21.74	1.61	0.964	19.14	3.97	0.998
S3	3.03	16.31	0.899	34.45	1.00	0.973	29.05	1.80	0.997
S4	2.72	17.34	0.908	40.73	0.80	0.975	33.43	1.33	0.996
BS1	3.44	12.50	0.919	23.80	1.25	0.976	20.94	1.65	0.956
BS3	2.56	17.46	0.915	44.11	0.68	0.966	36.10	0.76	0.981
M1	8.00	3.10	0.985	3.34	18.95	0.998	3.18	358.61	0.999
M2	4.73	3.84	0.981	4.40	9.36	0.979	3.94	215.84	0.952
M3	2.97	7.40	0.951	10.18	3.46	0.989	8.06	62.37	0.956
M4	2.86	10.02	0.930	14.02	3.29	0.987	11.21	42.79	0.987
BM3	2.19	10.88	0.934	18.80	1.65	0.968	14.69	5.75	0.961

where n has a value of $1/2$ to $2/3$. The n , q_m , K , and R^2 values for polymerized adsorbent with different amount of AMPS and AAm were calculated according to the nonlinear regression method, and are listed in Table 2. R^2 is a coefficient of determination that means more agreeable with approach to 1.0.

As shown in Fig. 5, the Langmuir and Sips models show better agreement than the Freundlich with the experimental data. In the case of the Langmuir isotherm, the adsorption behavior agrees well with the experimental data. However, a saturated amount of adsorption was predicted by the Langmuir model, which does not accord with the experimental data; the Sips model shows good agreement in this aspect. In general, the isotherm of protein adsorption is well fitted by the Sips model, because protein readily aggregated in the solution. In the case of the Langmuir adsorption model, it is assumed that the molecules are adsorbed with the monolayer [20]. Thus, adsorption of the protein by the multilayer in the aggregated proteins runs counter to the assumption of the Langmuir isotherm. Therefore, in the present work, all experimental data were fitted to the Sips model using the nonlinear regression method and the maximum adsorbed amount was predicted using this model.

Fig. 6 shows the effect of hydrophilic interaction on BSA adsorption with different amounts of hydrophilic AMPS and AAm in the adsorbent. As shown in the figure, the adsorbed amount of BSA increased with an increased amount of AMPS and AAm in the adsorbent. It could be concluded that the hydrophilic interaction governs the adsorption in these cases. If the hydrophobic interaction is dominant, the maximum adsorbed amount should decrease with an increasing amount of the hydrophilic group.

3.4. Effect of hydrophobic interaction on BSA adsorption

In this section, the change in adsorption capacity due to the appearance of hydrophobic BMA was examined for the S1, S3, and M4 polymers. In the case of polymer S4, even though the adsorbed amount was increased, it is not applicable to the microchannel, because AMPS, which has low solubility to the solvent, still exists in a solid state.

Kim et al. investigated the relationship between hydrophobic and electrostatic interactions in BSA adsorption with various sulfonated polystyrene microspheres and concluded that the hydrophobic interaction governed the adsorption in the low sulfonated microspheres, whereas electrostatic interaction did in high sulfonated ones [17,18].

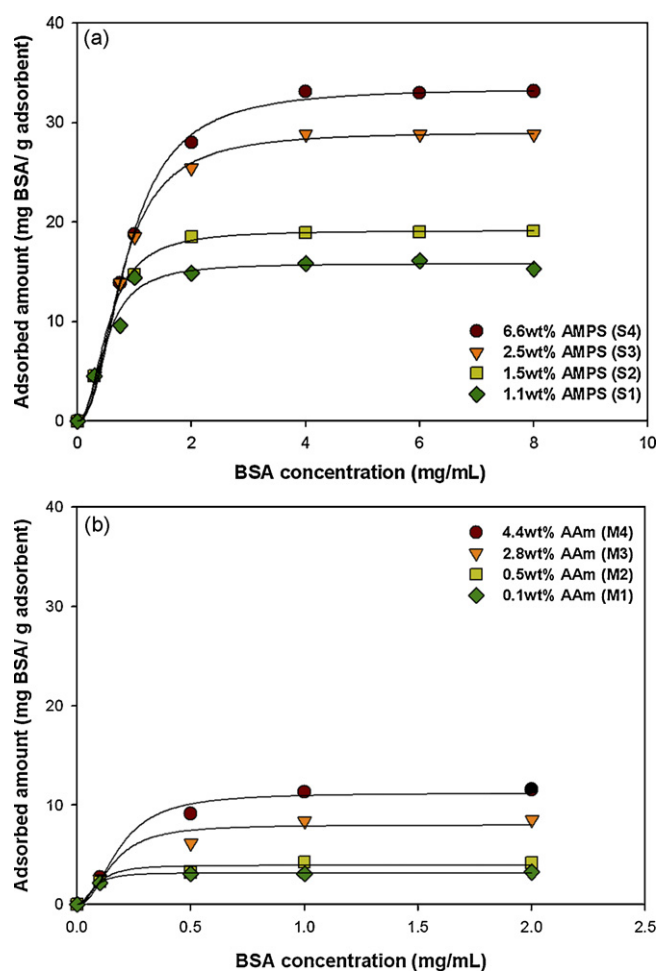


Fig. 6. Effect of hydrophilic interaction on BSA adsorption with different amounts of hydrophilic (a) AMPS or (b) AAm in adsorbents.

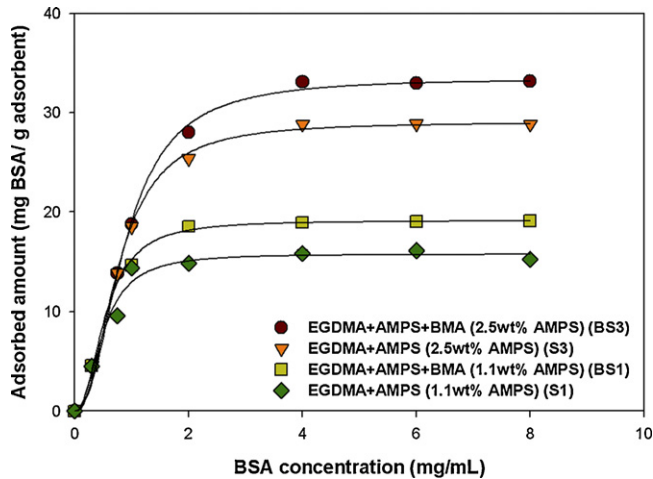


Fig. 7. Effect of hydrophobic interaction on BSA adsorption with addition of hydrophobic BMA to AMPS polymers.

In this study, as shown in Fig. 7, the adsorbed amount of BSA on adsorbent which was co-polymerized with hydrophobic BMA increased slightly compared to that on hydrophilic adsorbent. And the adsorbed capacity of AMPS–BMA copolymer was superior to that of AAm–BMA copolymer (data not shown). Fig. 8 shows the comparison of adsorbed amount on hydrophobic, hydrophilic and hydrophobic + hydrophilic adsorbents. Hydrophobic adsorbent is only co-polymerized BMA–EGDMA which is excepted AMPS from BS3 polymer. Hydrophilic adsorbent was S3 and hydrophobic + hydrophilic one is BS3. Adsorbed amount of BSA on each adsorbent showed the following order: hydrophobic + hydrophilic > hydrophilic > hydrophobic. Even though the amount of hydrophobic BMA increased in adsorbent, the adsorbed amount of BSA was not increased. Therefore, it could be concluded that the hydrophilic interaction governed the BSA adsorption compared to hydrophobic one and BS3 polymer had the maximum adsorbed capacity, 36 mg BSA per g adsorbent, in this experimental range. As a result of SPE in microfluidic

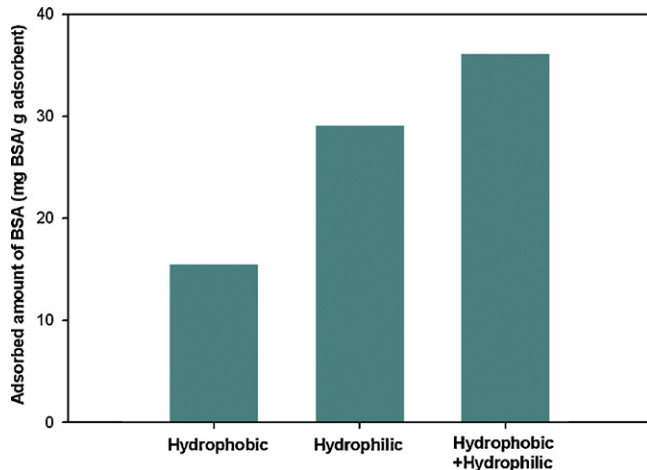


Fig. 8. Comparison of adsorbed amount on hydrophobic, hydrophilic, and hydrophobic + hydrophilic adsorbents.

device with BS3, there was no difference for the capacity of adsorbent between in bulk and microchannel (data not shown).

3.5. Selective removal of BSA in microchannel

In previous experiments, BSA was successfully removed in a microfluidic device. However, there are multi-components in real serum, and BSA could be co-extracted with biomarkers. Therefore, selective removal of BSA is required for the sample preparation step. The purpose of this experiment is to present the possibilities of selective removal and enrich the relatively low concentration of target materials with removal of the other ones to some degree. The objective of this experiment is to adsorb BSA onto the BS3 stationary phase while the adsorption of BGG should be minimized. BGG is a protein fraction of blood serum containing many antibodies to protect against bacterial and viral infectious diseases.

In this study, the isoelectric point, which is the native property of protein, is used for the selective removal of BSA. The maximum adsorbed amount of protein is usually observed around the isoelectric point. The isoelectric point of BSA is 4.8 and that of BGG is 6.5. Using these features, when SPE is performed at pH 4.5, selective removal should be possible [13]. The molecular weight of BSA is 64 kDa and that of BGG is known to 158 kDa. However, this is generally for a polymer form, and the molecular weight of the monomer is about 25 kDa. Thus, there are two

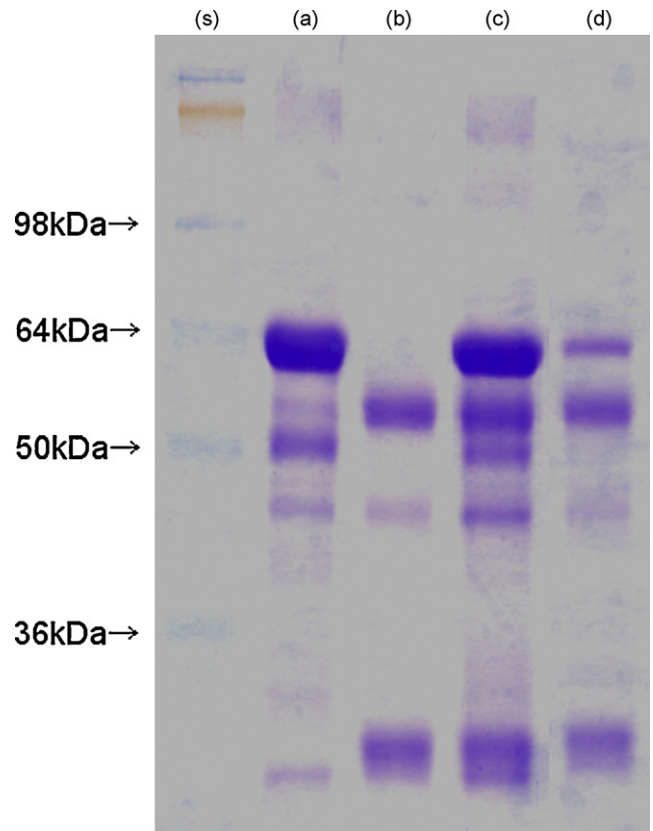


Fig. 9. SDS-PAGE of selective removal of BSA with BS3: (s) standard marker, (a) 1 mg/mL BSA, (b) 1 mg/mL BGG, (c) starting sample: BSA + BGG, (d) selective removal of BSA using SPE in microfluidic device.

bands in Fig. 9d, reflecting the monomer and dimer forms. Fig. 9 shows the purified protein from a bicomponent solution using SPE in a microchannel. In Fig. 9d, the band intensity of BSA at 64 kDa is clearly decreased compared to that of Fig. 9c. In the case of BGG, there is little change of intensity between Fig. 9c and d. As a result of analysis of SDS-PAGE intensity, it could be recognized that BSA was removed more than 40%, while BGG was removed less than 3%. And this result was not much decreased from the result of SPE in single component. Therefore, the selective removal of BSA via the adjustment of pH was successfully performed in a microfluidic device.

4. Conclusions

In this study, in order to determine the optimized conditions that could effectively facilitate removal of BSA in the microfluidic device, experiments to evaluate the effects of various parameters on BSA adsorption were carried out. By evaluating the effect of pH on BSA adsorption, the maximum adsorbed amount of BSA was observed around the isoelectric point. Under these pH conditions, the adsorption isotherms in accordance with the concentration of BSA solution and various hydrophilic monomers such as AMPS and AAm were examined. The adsorbed amount on a sulfonated stationary phase was found to be much larger than that on an aminated stationary phase. In the case of polymer BS3, which showed the maximum adsorbed amount of BSA, the adsorption capacity was 36 mg BSA/g adsorbent. In other studies, the maximum capacity of BSA adsorption on adsorbents which were polymerized with other method was 9 mg BSA/m² adsorbent [13,21]. Considering the specific surface area, adsorbent BS3 could treat 12 mg BSA/m² adsorbent which was exceeded in that of other methods.

Selective removal was performed in a bicomponent solution with BSA and BGG. The pH of the solution was adjusted to pH 4.5 to remove BSA selectively. The results were confirmed

with a SDS-PAGE. Finally, SPE as a sample preparation method in application of a micro total analysis system was successfully adapted to a microfluidic device.

Acknowledgements

This work was supported in part by MIC & IITA through IT Leading R&D Support Project.

References

- [1] D. Carter, J.X. Ho, *Adv. Protein Chem.* 45 (1994) 153.
- [2] C.F. Poole, *Trends Anal. Chem.* 22 (2003) 362.
- [3] A.H. El-Sheikh, A.A. Insisi, J.A. Sweileh, *J. Chromatogr. A* 1164 (2007) 25.
- [4] N.J.K. Simpson (Ed.), *Solid-Phase extraction*, Marcel Dekker, New York, 2000, p. 2.
- [5] K. Jinno, M. Taniguchi, M. Hayashida, *J. Pharmaceut. Biomed.* 17 (1998) 1081.
- [6] M. Volante, M. Pontello, L. Valoti, M. Cattaneo, M. Biauchi, L. Colzani, *Pest. Manage. Sci.* 56 (2000) 618.
- [7] H. Tian, A.F.R. Huhmer, J.P. Landers, *Anal. Biochem.* 283 (2000) 175.
- [8] F. Svec, J.M.J. Fréchet, *Science* 273 (1996) 205.
- [9] F. Svec, J.M.J. Fréchet, *Ind. Eng. Chem. Res.* 38 (1999) 34.
- [10] S. Xie, R.W. Allington, F. Svec, J.M.J. Fréchet, *J. Chromatogr. A* 865 (1999) 169.
- [11] E.C. Peters, M. Petro, F. Svec, J.M.J. Fréchet, *Anal. Chem.* 70 (1998) 2288.
- [12] C. Yu, F. Svec, J.M.J. Fréchet, *Electrophoresis* 21 (1999) 120.
- [13] J. Yoon, J.H. Lee, J. Kim, W. Kim, *Colloids Surf. B* 10 (1998) 365.
- [14] T. Rohr, D.F. Ogletree, F. Svec, J.M.J. Fréchet, *Adv. Funct. Mater.* 13 (2003) 264.
- [15] Y. Yang, C. Li, K.H. Lee, H.G. Craighead, *Electrophoresis* 26 (2005) 3622.
- [16] D.L. Pavia, G.M. Lampman, G.S. Kriz, *Introduction to Spectroscopy – A Guide for Students of Organic Chemistry*, second ed., Saunders, Fort Worth, TX, 1996, p. 31.
- [17] J. Yoon, J. Kim, W. Kim, *Colloids Surf. A* 153 (1999) 413.
- [18] J. Yoon, H. Park, J. Kim, W. Kim, *J. Colloid Interface Sci.* 177 (1996) 613.
- [19] R.A. Koble, T.E. Corrigan, *Ind. Eng. Chem.* 44 (1952) 383.
- [20] K. Kim, S. Kang, *J. Korean Ind. Eng. Chem.* 9 (1998) 311.
- [21] J. Hu, S. Li, B. Liu, *Biochem. Eng. J.* 23 (2005) 259.